International Journal of Thermal Sciences 49 (2010) 463–470

Contents lists available at ScienceDirect

International Journal of Thermal Sciences

journal homepage: www.elsevier.com/locate/ijts

A heat transfer parameter at air interfaces in the BLOCK model for building thermal environment

Jun Gao [a,*], Xu Zhang [a], Jia Ning Zhao [b], Fu Sheng Gao [b]

[a] Institute of HVAC&Gas Engineering, College of Mechanical Engineering, Tongji University, Shanghai 200092, China
[b] School of Municipal & Environmental Engineering, Harbin Institute of Technology, Harbin 150090, China

ARTICLE INFO

Article history:
Received 22 December 2008
Received in revised form
6 August 2009
Accepted 17 August 2009
Available online 29 August 2009

Keywords:
BLOCK model
Heat transfer factor
Thermal diffusion
Air layer
Thermal environment

ABSTRACT

A temperature-based zonal model (BLOCK model), proposed by Togari et al. [21], is improved in this study through determining a heat transfer factor between air layers. This factor has not been reasonably clarified and theoretically determined. Such shortage has long limited the applications of the model to building thermal environment and energy. In the present work, it is clarified to the combined laminar and turbulent diffusion of energy in the airflows. A physical definition is presented based on the one-dimensional thermal transport equation without advective and transient terms. Computational fluid dynamics (CFD) is used to calculate the values of the factor at air interfaces specified and to verify the physical definition. Calculated values are found to agree well with those assumed to reproduce the experimental data by Togari et al. [21], and are able to represent the thermal gradients observed in the experiments. This study intends to clarify and explain the nature of heat transfer factor between air layers in the BLOCK model and to promote its real applications.

1. Introduction

A zonal model is an intermediate approach between computational fluid dynamics (CFD) and multi-zone (single-room) models. It gives results faster than CFD and is more accurate than single-zone models. Various numerical methods have been recognized to be able to predict thermal environment at various levels of reliability and applications. A multi-zone model is based on the assumption that indoor air variables are homogeneous in each building zone. Its uniform assumption is a very poor approximation for the situation in a space with non-uniform air variables. The CFD goes to the other way round too complicated and time-consuming. Solving turbulence models requires fast computers with large amount of memory, especially for the cases where low-Reynolds-number thermally stratified flows are encountered in such spaces as atria and other spaces with stable thermal gradient. Dynamic CFD simulations for the thermal responses of buildings are very stiff and have been seldom tried in the literature except for the work by Moser et al. [18] and Chen et al. [6]. The reason is that room air has a characteristic time of a few or less seconds while building envelope has a few hours [23]. It leads to stiff calculation and huge time-consumption using a small time-step to account for the room air characteristics. It is therefore presently impracticable to perform unsteady CFD simulations for dynamic building thermal environment and energy. Comparatively, a zonal model exhibits more applicable for it disregards the turbulence and momentum transport and requires few computer resources for the calculation, because it is based on the small number of zones divided in the room space and the whole building envelopes, as the study by Griffith [10].

Allard and Inard [2] have extensively reviewed earlier zonal models. Megri et al. [16] reviewed the evolution of the zonal models, principally for single room analysis, used to design and control heating and cooling in the built environment, with emphasis on the development of models that designers and engineers can use to obtain a more accurate evaluation of building energy flows. Megri and Haghighat [15] reviewed the recent development and applications of zonal models for indoor environment. Two types of zonal model, the pressured-based and temperature-based, have been reported and categorized in the literature. Much work has been limited to the former, which applies the power-law equations to solve pressure field for the predicting of indoor airflow. A systematic attempt to use the zonal method with power-law equations to describe the airflow for various configurations in two dimensions is described in Wurtz et al. [22]; in that work convergence problems were encountered and the results did not agree well with measurements. It has been shown that this approach cannot correctly represent driving flows. Special laws for the special flows such as a jet and plume were applied to improve the convergence. However, the mass flow is modeled using pressure drop under a constant discharge coefficient in a pressure-based zonal

* Corresponding author. Tel.: +86 21 65984243.
E-mail address: gaojun-hvac@tongji.edu.cn (J. Gao).

1290-0729/$ – see front matter © 2009 Elsevier Masson SAS. All rights reserved.
doi:10.1016/j.ijthermalsci.2009.08.002

model, which was originally obtained from studies of flow through open doorways and was usually taken as 0.8 or 0.83 [10]. Axely [5] questioned such modeling formulation and showed that such coefficient introduces non-physical pressure drops. Song [20] found it failed to predict the temperature gradient due to the fact that the pressure difference based on a power law poorly represents the airflow driven by thermal effects in atria, when she integrated a pressured-based zonal model into the dynamic simulation tool DeST for a study of dynamic simulation of thermal environment in atria. Jiru and Haghighat [12] presented the discrepancies in applying the power law in the pressured-based zonal model and investigated that power law could not be improved by using the same discharge coefficient. They estimated the value of discharge coefficient for each cell to improve the prediction capability of the pressure-based zonal model. It should also be pointed out that the power law uses a square root of pressure drop and the large number of unknowns makes the solution numerically challenging.

Togari et al. [21] presented a temperature-based zonal model without the pressure drop and power law, i.e., the BLOCK model, which uses correlations on the basis of vertical temperature gradient in combination with special laws for jets and plumes. The temperature-based zonal model has less unknowns than the pressure-based one, and simpler in calculating. It is a good alternative to the pressure-based one, especially when only the information of temperatures are required. This model does not have to solve the pressure field and give good prediction of indoor thermal environment in the cases when thermal gradient exists, but not necessarily dominate. It is intended for evaluation of thermal environment in atria and those small rooms with displacement ventilation, under-floor air supply, stratification cooling and space heating with convective heaters. It has been recently applied by Huang et al. [11], Miura [17], and improved by Arai et al. [3] and Gao et al. [9]. However, there is also a tough problem with the BLOCK model, the indetermination of a heat transfer factor defined between air layers based on the temperature difference between layers. It was recognized by Togari et al. [21] that values of this factor had great influence on the prediction of indoor temperatures when some thermal gradient is formed and air mass transfer is suppressed. Only two empirical values, 2.3 W/m^2 K and 116 W/m^2 K, are suggested for positive and negative gradient of indoor vertical temperatures, respectively. In DOE-2 software, a similar empirical factor is set to 14.8 W/m^2 K [13]. Chow [7] used an empirical value of 10 W/m^2 K taken from the study by Achterbosch et al. [1] in his three-zone temperature stratification model in an atrium space. Griffith [10] indicated that the main problem with such a model is that it is difficult to arrive at a general-purpose coefficient for the convective heat transport terms at air layers as that widely applied for the wall and floor solid surfaces. Theoretical interpretation of such a parameter has never been reported. Actually, this kind of zonal model could be integrated into an unsteady-state one [3] and provide a promising tool for building thermal environment and energy simulation. It is therefore necessary to clarify the nature of heat transfer between air layers.

This study focuses on this factor in the BLOCK model and intends to give a reasonable definition for it. Numerical determination is presented using the CFD model. Experimental data are used to verify the present definition and validate the improved model.

2. A temperature-based zonal model – BLOCK model

For enclosures with overall or partial thermal gradient, a BLOCK model, has been proposed by Togari et al. [21] to predict the vertical temperature and thermal environment indoors. The building space considered is horizontally divided into a finite number of zones, layers or blocks, for each of which the temperature is assumed uniform. Airflow along wall surfaces, airflow due to thermal plume and jet, and air entrainment are modeled. Air mass and heat balances are established for each vertically divided zone. Airflow along vertical walls induced by the convective heat transfer and heat transfer between adjacent air layers are considered as the main force producing the pattern of thermal gradient in the space. Heat and air mass transfer through the wall boundaries are modeled using a wall current model. As described in Fig. 1, in this wall current model, heat convection drives mass flow $m_{\mathrm{out},i}$ from layer i to its related boundary layer with average temperature $t_{\mathrm{a},i}$. Assuming a turbulent boundary layer (Refer to Appendix A for the derivation of Eqs. (1) and (2)), we have

$$m_{\mathrm{out},i} = 4.00 h_{\mathrm{c},i} A_{\mathrm{w},i} / c_{\mathrm{p}} \tag{1}$$

$$t_{\mathrm{a},i} = 0.75 t_i + 0.25 \tau_{\mathrm{w},i} \tag{2}$$

where, h_{c} is the convection coefficient, which can be determined by various correlations from the experiments for building energy in the literature [4], and it could also be decided by those empirical coefficients widely used in the building energy programs; A_{w} is wall surface area; τ_{w} is wall surface temperature, which can be derived by

$$\tau_{\mathrm{w},i} = q_{\mathrm{w}} / h_{\mathrm{c},i} + t_i \tag{3}$$

As described by Eq. (4), airflow from the boundary layer within a lower layer $i-1$ will combine the airflow from layer i to form a total airflow, $m_{\mathrm{T},i}$, whose average temperature is evaluated by Eq. (5). Before this combined airflow enters the next layer $i+1$, some part, caused by the relative temperature between the adjacent layers, should be decomposed and flow back to layer i. Table 1 shows the judgment of this kind of backflow. Fig. 1 also shows such composition and decomposition in the wall current model.

$$m_{\mathrm{T},i} = m'_{\mathrm{T},i-1} + m_{\mathrm{out},i} \tag{4}$$

$$t_{\mathrm{T},i} = \frac{m'_{\mathrm{T},i-1} t_{\mathrm{T},i-1} + m_{\mathrm{out},i} t_{\mathrm{a},i}}{m_{\mathrm{T},i}} \tag{5}$$

Different jet and plume models can be integrated to evaluate the effect of special flows on the indoor thermal gradient. Air mass balance in layer i is represented by

$$m_i - m_{i+1} + m_{\mathrm{in},i} - m_{\mathrm{out},i} - m_{\mathrm{P},i} = 0 \tag{6}$$

where, $m_{\mathrm{P},i}$ is the entrained air mass by the plume (or jet) within layer i, and is subtractive since it departs from layer i; m_i and m_{i+1} denotes air mass between adjacent layers through their interfacial boundary. The flow direction is assumed upward, so m_i is positive and m_{i+1} is subtractive. Moreover, $m_{\mathrm{out},i}$ and $m_{\mathrm{in},i}$ are airflow departing from and back to layer i along the boundary layer, respectively. Therefore, they

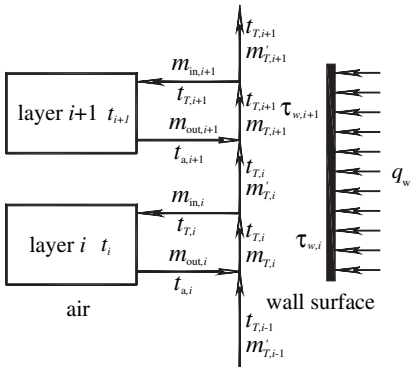

Fig. 1. Wall current model in the temperature-based zonal model.

Table 1
Judgment of backflow along vertical walls.

Conditions	Mass flow
$t_{T,i} < t_i$	$m_{in,i} = m_{T,i}, \quad m'_{T,i} = 0$
$t_i \le t_{T,i} \le t_{i+1}$	$m_{in,i} = \frac{m_{T,i}(t_{i+1} - t_{T,i})}{t_{i+1} - t_i}, \quad m'_{T,i} = m_{T,i} - m_{in,i}$
$t_{T,i} > t_{i+1}$	$m_{in,i} = 0, \quad m'_{T,i} = m_{T,i}$

are subtractive and positive in the mass balance, respectively. From this modeling approach, airflow is driven by the heat convection at wall surfaces and its composition/decomposition is judged by the buoyancy effect. Air mass flow between layers, m_i, is directly resolved through Eq. (6) and is not calculated by the pressure difference based on a power law. Heat balance in layer i is

$$w_1 c_p m_i (t_{i-1} - t_i) + w_2 c_p (-m_{i+1})(t_{i+1} - t_i) + c_p m_{in,i}(t_{T,i} - t_i) + c_{b,i} A (t_{i+1} - t_i) + c_{b,i-1} A (t_{i-1} - t_i) = 0 \quad (7)$$

where, $w_1 = 0$ when $m_i < 0$, and $w_1 = 1$ when $m_i \ge 0$; $w_2 = 1$ when $m_{i+1} < 0$, and $w_2 = 0$ when $m_{i+1} \ge 0$; c_b is the heat transfer factor between adjacent air layers. Here t_i is the unknown to be finally obtained from the heat balances.

Using Eqs. (6) and (7), the BLOCK model is to reproduce the thermal gradient and airflow in the building space. However, the nondeterminacy of c_b remains as one problem.

3. Definition of the factor

A physical definition of the heat transfer factor is required before some quantitative work could be used to calculate its values. According to its role in the model, it is obviously not used to represent the heat transfer produced by air mass exchange at the interfaces because this transfer has been calculated through Eq. (7). It exhibits the characteristics of heat transfer along wall surface as the coefficient of heat convection. Just like the heat transfer at the boundary layer, this factor first acts as the conductive heat transfer through the air due to the fact that temperature changes monotonically at each air interface. Local turbulence intensifies such heat transfer through the turbulent conduction. Therefore, the heat transfer concerned is subject to the combined laminar and turbulent diffusion of energy, i.e., thermal effective diffusion. Effective diffusion in the airflow is unrelated to the advective and transient effect, and it can be represented by the right hand of the following equation with the diffusion coefficient Γ_{eff}

$$\frac{\partial \rho t}{\partial \tau} + \frac{\partial \rho U t}{\partial X} = \frac{\partial}{\partial X}\left(\Gamma_{eff} \frac{\partial t}{\partial X}\right) \quad (8)$$

where, U and X denote the velocity component and coordinate directions, respectively. Γ_{eff} is the effective diffusion coefficient, $\Gamma_{eff} = \mu/\mathrm{Pr} + \mu_t/\mathrm{Pr}_t = \lambda/c_p + \mu_t/\mathrm{Pr}_t$. μ and μ_t are the molecular and turbulent viscosity, respectively. Pr and Pr_t are the molecular and turbulent Prandtl number, respectively. λ is the thermal conductivity of air. c_p is the heat capacity of air. One-dimensional heat transfer between adjacent air layers can be represented by the effective conduction in the airflow as

$$q_b \left(\lambda + \frac{c_p \mu_t}{\mathrm{Pr}_t}\right) \frac{\partial t}{\partial y} \quad (9)$$

When a characteristic length l is introduced, the physical definition of c_b, as a heat transfer factor, can simply be

$$c_b = \frac{q_b}{\Delta t} = \frac{\lambda}{l} + \frac{c_p \mu_t}{\mathrm{Pr}_t l} \quad (10)$$

This length is defined to be the depth of a local zone in the zonal model (0.5 m as suggested by [9]). Heat transfer between air layers can then be the effective thermal conductivity divided by the zone depth. If we introduce the laminar viscosity as $c_b = \mu[\lambda/\mu l + c_p(\mu_t/\mu)/\mathrm{Pr}_t l]$ and keep in mind that only c_b and μ_t/μ are unknown (Here Pr_t is generally 0.85), then value of c_b keeps a linear relationship with the turbulent viscosity ratio as Fig. 2. Thus, the value of 2.3 W/m^2 K corresponds to a low turbulent viscosity ratio of 53, which means significantly attenuated turbulence for indoor airflows. At a moderate level of turbulence, e.g., $\mu_t/\mu = 470$, this value may reach up to 20 W/m^2 K, which represents somewhat intensive convection for indoor airflows. It is also observed the heat transfer factor may be very small for laminar or near-laminar flows (See the values of c_b when $\mu_t/\mu << 1$ in Fig. 2).

Obviously, both h_c and c_b are convective coefficient. h_c is defined as the convective heat transfer at the wall surfaces, and c_b is at air interfaces. h_c is affected by the attenuated turbulence near the wall. c_b represents the heat transfer between air layers with the turbulence level at the air interfaces.

4. Verification and validation

4.1. Experimental setup

To verify the physical definition of c_b and validate the improved BLOCK model, experimental data by Togari et al. [21] using a chamber 3 m × 3 m × 2.5 m (height) (see Fig. 3) are used. This chamber was located in an airflow test laboratory. The test room was made entirely of insulated boards, with the exception of one wall, which was made of glass. An air supply outlet was mounted in the wall opposite to the glass wall and 625 mm above the floor. A return inlet was installed at the bottom of the same wall, 250 mm above the floor. Interior air, and interior and exterior surface temperatures were measured using Cu–Co thermocouples at 160 locations on the symmetry and its perpendicular plane, as shown in Fig. 3. Heat flow sensors covered with aluminum foil were also used to measure heat flux on wall surfaces. Internal surface temperatures from the experiments are applied as the boundary conditions (see Fig. 4). The convective heat transfer coefficient h_c was mainly determined by the measured surface heat flux and surface temperatures through $h_c = q/\Delta t$. It is also improved by evaluating the effect of surface-to-surface heat radiation. Values of h_c are obtained as follows.

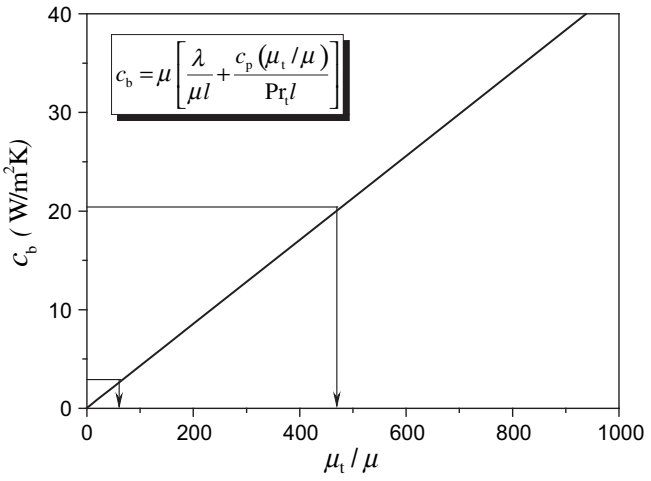

Fig. 2. Linear relationship between the heat transfer factor and turbulent viscosity ratio.

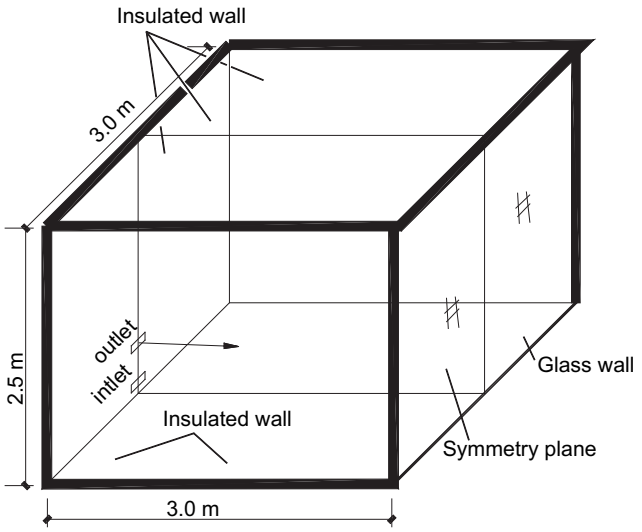

Fig. 3. Configuration of the experiment by Togari et al. [21].

1) For case a (natural convection), h_c is 3.5, 2.3 and 4.6 W/m^2 K at the vertical walls, floor and ceiling, respectively.
2) For case b (low-level cool air supply), h_c is 9.3 W/m^2 K at the floor and vertical walls in the lower zones affected by cool jet, 5.8 W/m^2 K at other parts of the vertical walls affected by cool jet, 3.5 W/m^2 K at other vertical walls, and 4.6 W/m^2 K at the ceiling.

Interior air temperatures are used to verify and validate the present work. Other sets of the experiments are assembled in Table 2.

4.2. Numerical determination

Quantitative work of the factor is necessary and it should be able to correspond to the physical definition as Eq. (10). Turbulent viscosity in Eq. (10) is really phenomenological and not measurable as the molecular viscosity and it should be calculated from other turbulent parameters that can be directly measured. Without direct precision measurements of indoor air turbulence, the CFD method can, however, provide the detailed information for the calculation of c_b. At present, the key task has been the evaluation of the physical definition. In the case that CFD is validated to give reliable prediction, it should be useful to give the c_b values.

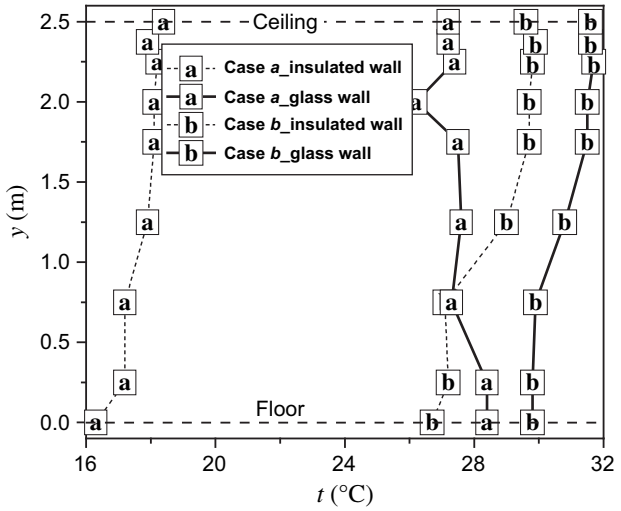

Fig. 4. Surface temperatures measured in experiment.

Table 2
Experimental sets for the cases considered, from Togari et al. [21].

	Outlet size	Air volume of supply	Air supply temperature	Momentum
Case a	Natural convection, glass wall heated			
Case b	250 mm × 74 mm	100 m^3/h	13.8 °C	0.052 kg/s^2
Case c	500 mm × 74 mm	150 m^3/h	40.7 °C	0.053 kg/s^2
Case d	250 mm × 74 mm	135 m^3/h	12.1 °C	0.095 kg/s^2

For indoor airflows with turbulence attenuated in the core region due to vertical thermal gradient in our present study, an improved low-Reynolds RNG k–ε model together with an improved non-equilibrium wall function (See Appendix B) are adopted. This RNG model is endeavored to well represent the effect of indoor low-Re flows due to vertical thermal gradient, and have been widely validated through experimental and LES data. Pressure-velocity coupling for the numerical solution is achieved by using the SIMPLE algorithm [19]. The three-order QUICK differencing scheme [14] is used to discretize the advection terms for Navier–Stokes equations, the energy equations and the turbulent transport equations. Only half of the chamber domain is modeled with a plane of symmetry identified in the geometry (see Fig. 3). Grid-independent solution is tested using different grid sizes. The final grid used is presented as Fig. 5, whose boundary increment ratio is 1.5 with the first grid size 0.005 m and maximum space grid size 0.2 m.

From the CFD meshes, the heat transfer concerned can be illustrated by Fig. 5 and the heat transfer factor expressed by Eq. (10) is therefore derived as

$$c_b = \frac{\frac{1}{n}\sum_{k=1}^{n}\left[\frac{\Delta t_\delta}{\delta}\left(\lambda + c_p\mu_t/\mathrm{Pr}_t\right)\right]_k}{(t_{i+1} - t_i)} \tag{11}$$

where, $\Delta t_\delta/\delta$ is the local temperature gradient in the CFD; t_{i+1} and t_i are zone or block temperatures derived by averaging at all related nodes in the CFD (based on the zone depth). If the grid size is different from the zone depth in the zonal model, interpolation should be used to calculate the zone temperature. Eq. (11) is applied to the cases

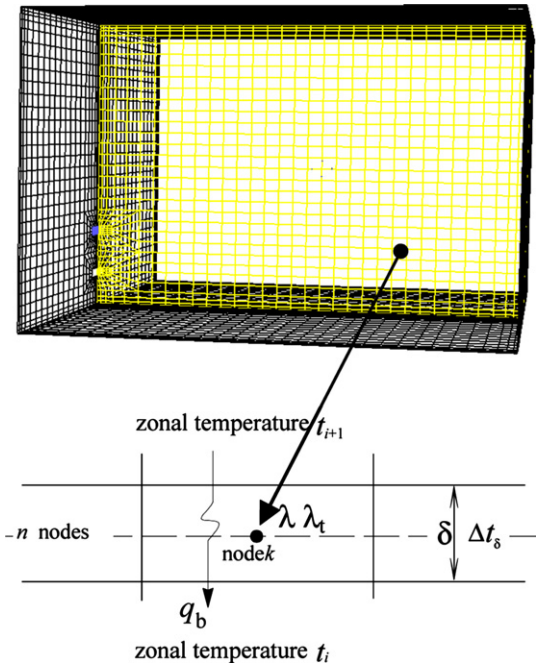

Fig. 5. CFD meshes and the numerical determination of heat transfer factor c_b.

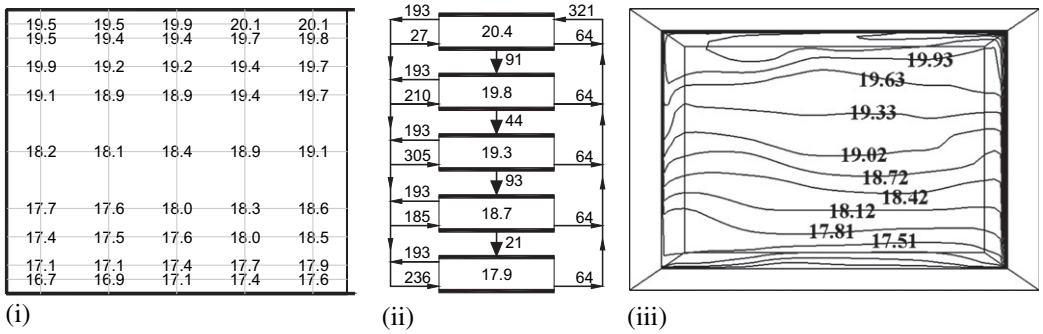

Fig. 6. Comparison of the results of thermal gradient for Case a, (i) Experimental result, Togari et al. [21], (ii) Result by BLOCK model ($c_b = 2.3$ W/m^2 K), Togari et al. [21], (iii) CFD result.

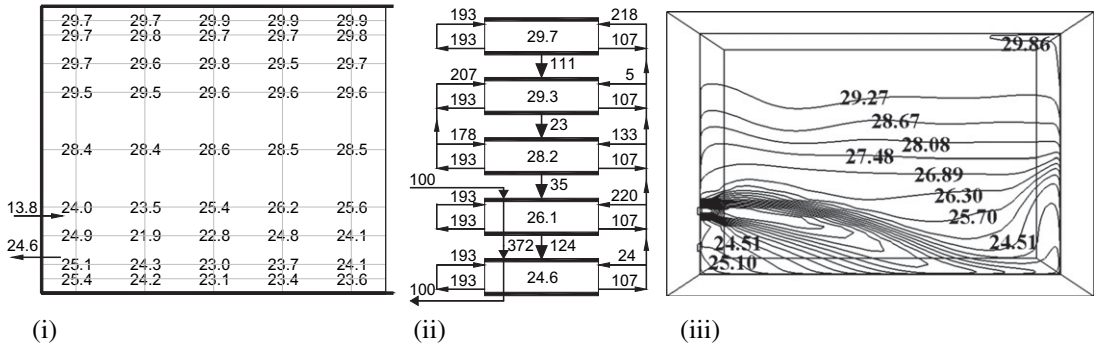

Fig. 7. Comparison of the results of thermal gradient for Case b, (i) Experimental result, Togari et al. [21], (ii) Result by BLOCK model ($c_b = 2.3$ W/m^2 K), Togari et al. [21], (iii) CFD result.

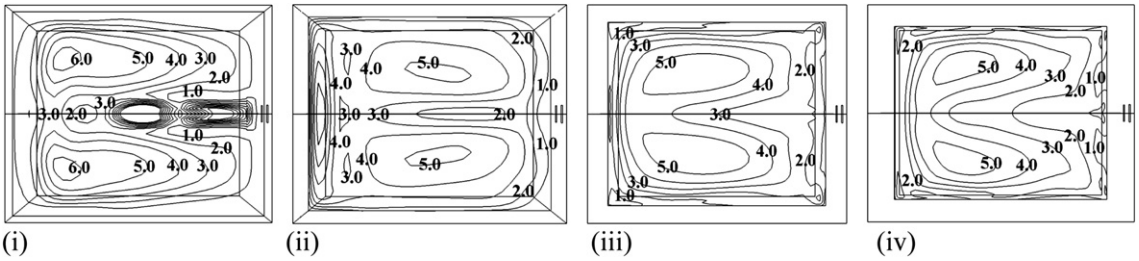

Fig. 8. Distribution of c_b at four horizontal interfaces for Case b (c_b calculated by Eq. (10)), (i) Horizontal interface plane at $y = 0.5$ m, (ii) Horizontal interface plane at $y = 1.0$ m, (iii) Horizontal interface plane at $y = 1.5$ m, (iv) Horizontal interface plane at $y = 2.0$ m.

where the meshes are uniform. When the meshes are non-uniform, c_b values can be averaged at each node through weighting by the horizontal area of each cell at the interfaces. A user-defined function is used to calculate the c_b values at the CFD platform.

4.3. Results and comparisons

Predicted results of indoor thermal gradients by the BLOCK model (with assumed value $c_b = 2.3$ W/m^2 K, it is also calculated by [21] and CFD, and their comparisons with the experimental data are presented in Figs. 6 and 7. Figs. 6(i) and 7(i) give the temperature distribution of experimental data by Togari et al. [21], for cases a and b, respectively; Figs. 6(ii) and 7(ii) provide the predicted vertical temperature distribution and airflows by BLOCK model; Figs. 6(iii) and 7(iii) presents the indoor temperature distribution in the plane of symmetry by the CFD. As Fig. 6 shown, indoor thermal gradient for case a is driven by the heat flux from the glass wall heated and the experimental data provided are the averaged temperature of measuring points at the same level. As Fig. 7 shown, indoor thermal gradient for case b is achieved by the low-level cool air supply in the space and the temperature difference between air supply and interior wall surfaces. See Figs. 6 and 7, the space is uniformly divided into five zones for the calculation of zonal model. To verify the assumed empirical values, BLOCK model is first resolved using the generally assumed $c_b = 2.3$ W/m^2 K to reproduce the thermal gradient (See Figs. 6(ii) and 7(ii)), as the work by Togari et al. [21]. In this situation, the CFD method represents well the thermal gradients and BLOCK model with the assumed value of c_b provisionally reproduces the experimental results. However, this general value of c_b was decided by attempts to reproduce the experimental data of

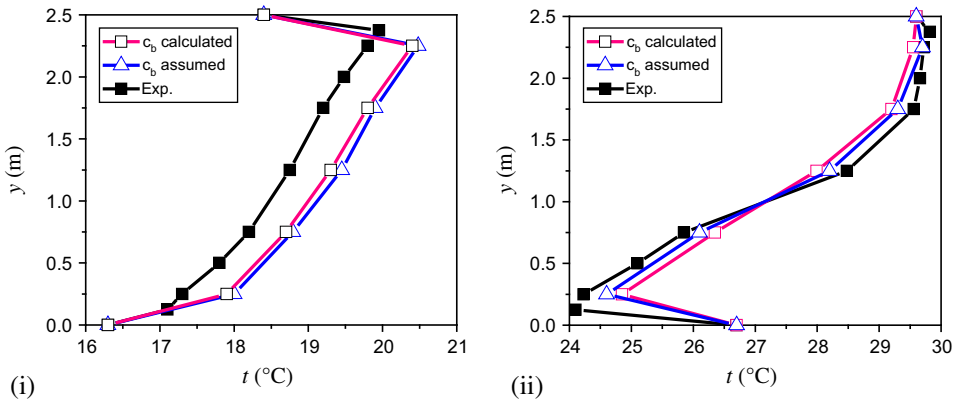

Fig. 9. Comparisons of vertical temperature profiles under different c_b values, (i) Case a, (ii) Case b.

vertical temperature profiles, but not theoretically and reasonably decided. Therefore, it is still pendent with a guess value.

c_b values at the four interfaces are thereafter calculated using Eq. (11). Distribution of c_b can be directly obtained and plotted on the CFD platform. In case a, the value of c_b is very uniform throughout the horizontal interface and its mean value is 2.1–2.8 W/m^2 K at different levels specified, which is close to the assumed value. In case b, the mean value is 2.7–3.7 W/m^2 K. Fig. 8 presents the distribution of c_b at four horizontal interfaces for Case b, calculated by the CFD. The area-weighted mean values can be obtained at four interfaces, which are 3.7, 3.4, 3.2 and 2.7 W/m^2 K, respectively. Higher values are observed at the interfaces near the level of air supply where turbulent diffusion is significantly increased by the cool jet. Conversely, lower values are found at the interfaces where turbulent thermal diffusion is lower and thermally stratified flows dominate. The calculated c_b reflects that heat transfer between air layers is influenced by the turbulent level of local airflow as described in Fig. 2. Values of c_b for case b in Fig. 8 are fed to BLOCK model, replacing the assumed $c_b = 2.3$ W/m^2 K, to calculate the vertical temperatures. New results and their comparisons with the experimental data are presented in Fig. 9 where the vertical profiles of indoor air temperature are predicted by BLOCK model using the assumed c_b value and calculated value, respectively. The heat transfer factor calculated produces similar results to those by the assumed value. The assumed empirical value appears good because it is decided by an attempt to keep the predicted results close to experimental data and it is very close to real values. It is confirmed that the present definition of c_b is reasonable and its calculated values are able to represent the heat transfer between adjacent air layers in the BLOCK model.

5. Further confirmation

Two other cases are considered to further validate the improved model with the c_b values calculated based on its definition. Experimental data are obtained from Togari et al's work [21]. In case c, hot air of 40.7 °C and 150 m^3/h is supplied at a lower inlet and returned at a higher outlet, and air volume moves upward in the space with a cold glass wall to produce a large thermal gradient. In case d, cool air of 12.1 °C and 135 m^3/h is supplied and returned at the lower part of the space with a hot glass wall, air volume is settled in the lower space to produce a significant indoor thermal gradient. Two cases represent space heating and cooling in different seasons using air conditioning, respectively.

Averaged values of c_b at four levels for the two cases and the predicted thermal gradients using these values are presented in Fig. 10. Averaged values of c_b are fed by the CFD and their differences are shown at the right vertical coordinates in Fig. 10. By analyzing the trajectory of hot/cool jet, one can relate a higher value of c_b to a higher level of turbulence. It corresponds to the physical definition of c_b as Eq. (10). From the comparisons in Fig. 10, the results of improved BLOCK model agree well with the measurements. The heat transfer factor does successfully represent the effective thermal diffusion in the airflows under thermal gradients driven by space heating and cooling. It gives confidence to assess the indoor thermal environment with occupied conditioning by applying the settled model in the near future when a database for c_b (as that for convective coefficients along building walls) is completed with the measurement of turbulence distribution or by calculating tools, such as the CFD.

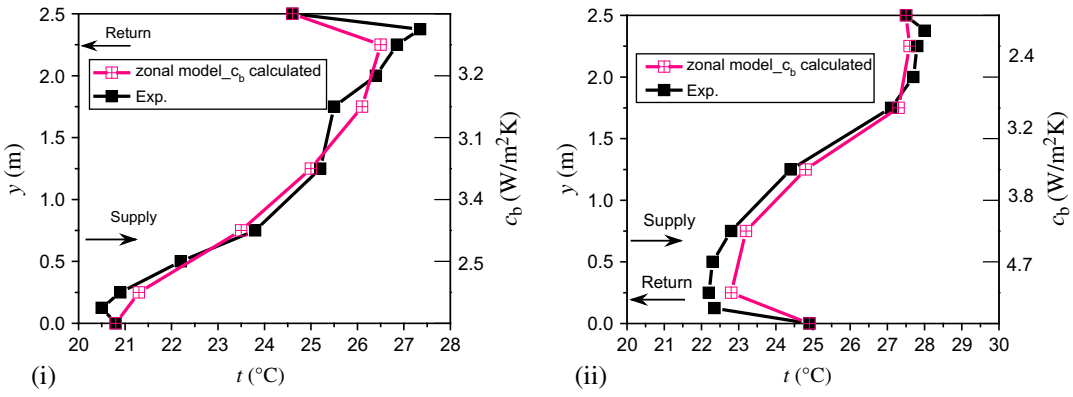

Fig. 10. Comparisons of vertical temperature profiles predicted by BLOCK model with experimental data from Togari et al's work [21], (i) Case c, (ii) Case d.

6. Conclusions

This study clarifies and explains the heat transfer factor between air layers in the BLOCK model. The factor is now defined to represent the heat transfer per unit area and temperature difference between adjacent air layers due to the combined diffusion of laminar and turbulent conduction. A theoretical equation is established based on this definition. The CFD method is presently used to calculate the values of the factor and verify the definition related to the local mean turbulent level. The present definition is proved reasonable based on the result that the values are capable of reproducing the experimental data. The performance of the BLOCK model could therefore be improved.

It is really pendent how to simply derive the values of this factor when different indoor airflows are encountered. Actually, much distinct values (relative difference may reach up to 600 times in a single space) have been found in our other work. Much work should be performed to assess the sensitivity of the predicted results to the heat transfer factor, and to further establish a database/expressions (just as the convection coefficients along walls used in the program of building energy) responding to the indoor airflows driven by the typical ways of air-conditioning, ventilating and heating. It is not practical that one does a CFD simulation for the calculation of BLOCK model every time. From this work, it is expectable to use the CFD simulations or precision measurements of indoor air turbulence to establish a database responding to varied airflows and to guide the application of BLOCK model to actual indoor thermal environment in the near future. However, turbulent viscosity is phenomenological and not measurable as the molecular viscosity, and should be evaluated from other turbulent parameters that can be directly measured. Therefore, the CFD is presently a simple method to produce a database of the heat transfer factor for engineering applications.

Acknowledgment

This work was supported by the National Science Foundation for Post-doctoral Scientists of China (Grant No.20070420111) and State Key Laboratory of Pollution Control and Resource Reuse Foundation, China (No.PCRRF09009). Authors are very grateful to the reviewers for their valuable comments for improving this article for publication.

Appendix A. Derivation of Eqs. (1) and (2)

According to the boundary-layer theory in Eckert and Jackson [8], as presented by Togari et al. [21], turbulent free convection along flat plate can has the following velocity and temperature profiles (1/7-law) in the boundary layer.

$$\frac{u}{u_\infty} = \left(\frac{y}{\delta_t}\right)^{1/7}\left(1-\frac{y}{\delta_t}\right)^4 \tag{A1}$$

$$\frac{|t-\tau_w|}{\Delta\tau_w} = \left(\frac{y}{\delta_t}\right)^{1/7} \tag{A2}$$

where, u and t are the velocity and temperature in the boundary layer, respectively; δ_t the thickness of thermal boundary layer; u_∞ and τ_w are the velocity in the main field and wall surface temperature, respectively; $\Delta\tau_w$ is the temperature difference between air in the main field and wall surface; y is the distance to wall surface. To calculate the averaged temperature of air in the boundary layer t_a, the following method is used

$$t_a = \frac{\int_0^{\delta_t} ut\,dy}{\int_0^{\delta_t} u\,dy} \tag{A3}$$

Substitute Eqs. (A1) and (A2) into Eq. (A3), we have the following for a layer i in the BLOCK model

$$t_{a,i} = 0.75t_i + 0.25\tau_{w,i} \tag{A4}$$

where, t_i is the air temperature in layer i. Along the boundary layer, a mass flow m_{out} from layer i is driven by the heat convection at the wall surface, then

$$c_p m_{out,i}(t_{a,i}-t_i) = h_{c,i}A_{w,i}(\tau_{w,i}-t_i) \tag{A5}$$

where, h_c is the convection coefficient; A_w is wall surface area. Substitute Eq. (A4) into Eq. (A5), we have

$$m_{out,i} = 4.0h_{c,i}A_{w,i}/c_p \tag{A6}$$

Appendix B. Turbulence model and wall functions used

Table B1. An improved RNG k–ε model for indoor thermally stratified flows.

k and ε equation	$\rho\frac{\partial k}{\partial t}+\rho\frac{\partial(ku_i)}{\partial x_i} = \frac{\partial}{\partial x_j}\left[\left(\frac{\mu+\mu_t}{\sigma_k}\right)\frac{\partial k}{\partial x_j}\right]+G_k+G_b-\rho\varepsilon$
	$\rho\frac{\partial \varepsilon}{\partial t}+\rho\frac{\partial(\varepsilon u_i)}{\partial x_i} = \frac{\partial}{\partial x_j}\left[\left(\frac{\mu+\mu_t}{\sigma_\varepsilon}\right)\frac{\partial \varepsilon}{\partial x_j}\right]+C_1\frac{\varepsilon}{k}G_k-C_2\rho\frac{\varepsilon^2}{k}$
Turbulent Prandtl numbers	$\left\lvert\frac{\alpha-1.3929}{0.3929}\right\rvert^{0.6321}\left\lvert\frac{\alpha+2.3929}{1.3929}\right\rvert^{0.3679} = \frac{\mu}{\mu+\mu_t}$, $\mathrm{Pr}_t = \begin{cases}0.85\frac{(1+1.33\mathrm{Ri})^{1.5}}{(1+10\mathrm{Ri})^{0.5}}, & \mathrm{Ri}\ge 0\\ 0.85, & \mathrm{Ri}<0\end{cases}$
Turbulent viscosity, damping function	$\mu_t = C_\mu\rho f_\mu k^2/\varepsilon$, $f_\mu = f'_\mu f''_\mu$
	$f'_\mu = \exp\left[\frac{-0.30}{(0.20+\mathrm{Re}_t/65.25)^{2.5}+0.06}\right]\exp(1.00/\mathrm{Re}_t)$ $f''_\mu = \begin{cases}(1.37-0.37P_k/\varepsilon+1.6G_k/\varepsilon)^{1-\exp(-30\mathrm{Ri})}, & \mathrm{Ri}\ge 0\\ 1.0, & -2\le\mathrm{Ri}<0\\ 1.283(1-0.239\mathrm{Ri}\eta), & \mathrm{Ri}<-2\end{cases}$
Model constants	$C_1 = 1.42$, $C_2 = 1.68+\frac{C_\mu\eta^3(1-\eta/4.38)}{1+0.012\eta^3}$, $C_\mu = 0.0845$,

where, G_b and G_k are the generation of turbulence kinetic energy due to buoyancy and mean velocity gradient, respectively. σ_k and σ_s are the turbulent Prandtl numbers for k and ε, respectively (the inverse effective Prandtl numbers from α, derived by the RNG theory). μ_t and μ are the turbulent and molecular viscosity, respectively. ρ is the air density. η is defined by $\eta = Sk/\varepsilon$, and $S=(2S_{ij}S_{ij})^{0.5}$, $S_{ij} = 0.5(\partial u_i/\partial x_j+\partial u_j/\partial x_i)$. Turbulent Reynolds Re_t is defined by $\rho k^2/\mu\varepsilon$. Flux Richardson number $\mathrm{Ri} = -G_b/G_k$ Model constants are dynamically derived by using the RNG theory.

Table B2. Hybrid non-equilibrium wall functions used in this work.

Near-wall temperature and velocity function	$\tilde{U}^+ = \begin{cases} 0.00477y^+\exp(30/y^+), & y \le 0.5y_v \\ y^+, & 0.5y_v < y < y_v \\ \frac{1}{\kappa}\ln(Ey^+), & y \ge y_v \end{cases}$ $T^+ = \frac{(T_w - T_p)\rho c_p C_\mu^{1/4} k_p^{1/2}}{q_w} = \begin{cases} \mathrm{Pr}y^+, & y^+ < y_T^+ \\ \frac{\mathrm{Pr}_t}{\kappa}\ln(Ey^+) + \mathrm{Pr}_t P, & y^+ \ge y_T^+ \end{cases}$
Near-wall shear stress, k and ε profile	$\tau_t = \begin{cases} 0, & y < y_v \\ \tau_w, & y \ge y_v \end{cases}$, $k = \begin{cases} \left(\frac{y}{y_v}\right)^2 k_p, & y < y_v \\ k_p, & y \ge y_v \end{cases}$, $\varepsilon = \begin{cases} \frac{2\mu k}{\rho y^2}, & y < y_v \\ \frac{k^{3/2}}{\kappa C_\mu^{-3/4} y}, & y \ge y_v \end{cases}$,
Non-dimensional velocity, temperature,	$\tilde{U}^+ = \frac{U^+}{u_p}\left\{u_p - \frac{1}{2}\frac{dp}{dx}\left[\frac{y_v}{\rho\kappa\sqrt{k}}\ln\left(\frac{y}{y_v}\right) + \frac{y - y_v}{\rho\kappa\sqrt{k}} + \frac{y_v^2}{\mu}\right]\right\}$ $U^+ = \frac{u_p C_\mu^{1/4} k_p^{1/2}}{\tau_w/\rho}$, $y^+ = \frac{y_p \rho C_\mu^{1/4} k_p^{1/2}}{\mu}$
Model constants	$y_T^+ \approx y_v^+ = 11.225$, $\kappa = 0.4187$, $E = 9.793$, $\mathrm{Pr}_t = 0.85$

where, the subscript **p** denotes the point at the cell center adjacent to wall. The subscript **w** denotes wall. y_v is physical viscous sublayer thickness. τ is shear stress. Near-wall shear stress, k and ε profile apply the two-layer conception to compute the budget of turbulence kinetic energy at the wall-adjacent cells, which is needed to solve the k equation at the wall-neighboring cells. The wall-neighboring cells are largely assumed to consist of a viscous sublayer and a fully turbulent layer except for ε, which is calculated directly by $\varepsilon_p = 0.476(k_p)^{1.5}/y$ when $y < 0.5y_v$.

References

[1] G.G.J. Achterbosch, P.P.G. Jong, C.E. Krist-Spit, S.K. Van der Meulen, J. Verberne, The development of a convenient thermal dynamic building model, Energy and Buildings 8 (1985) 183–196.

[2] F. Allard, C. Inard, Natural and mixed convection in rooms: prediction of thermal stratification and heat transfer by zonal models, in: Proceedings of International Symposium of Room Air Convection and Ventilation Effectiveness, Tokyo, Japan, 1992, pp. 335–342.

[3] Y. Arai, S. Togari, K. Miura, Unsteady-state thermal analysis of a large space with vertical temperature distribution, ASHRAE Transactions 100 (part 1) (1994) 396–411.

[4] ASHRAE Fundamental, American Society of Heating, Refrigeration, and Air Conditioning Engineers, Inc., Atlanta, 2001.

[5] J.W. Axley, Surface-drag flow relations for zonal modeling, Building and Environment 36 (2001) 843–850.

[6] Q. Chen, X. Peng, A.H.C. van Paassen, Prediction of room thermal response by CFD technique with conjugate heat transfer and radiation models, ASHRAE Transactions 101 (1995) 50–60.

[7] W.K. Chow, Assessment of thermal environment in an atrium with air-conditioning, Journal of Environmental Systems 25 (4) (1997) 409–420.

[8] E.R.G. Eckert, T.W. Jackson, Analysis of turbulent free-convection boundary layer on flat plate, NACA Report 1015, 1951.

[9] J. Gao, J. Zhao, X. Li, F. Gao, A zonal model for large enclosures with combined stratification cooling and natural ventilation: part 1—model generation and its procedure, Journal of Solar Energy Engineering–Transactions of the ASME 128 (2006) 367–375.

[10] B.T. Griffith, Incorporating Nodal and Zonal Room Air Models into Building Energy Calculation Procedures, Master of Science Thesis, Massachusetts Institute of Technology, 2002.

[11] C. Huang, Y. Song, X. Luo, Application of the Gebhart-BLOCK model for predicting vertical temperature distribution in a large space building with natural ventilation, Maximize Comfort: temperature, Humidity and IAQ, vol. I-8–1, Proceedings of the ICEBO2006, Shenzhen, China, 2006.

[12] T.E. Jiru, F. Haghighat, A new generation of zonal models, ASHRAE Transactions 112 (2) (2006) 163–174.

[13] D.R. Landsberg, H.P. Misuiello, S. Moreno, Design strategies for energy-efficiency atrium spaces, ASHRAE Transactions 92 (2) (1986) 310–328.

[14] B.P. Leonard, S. Mokhtari, ULTRA-SHARP Nonoscillatory Convection Schemes for High-speed Steady Multidimensional Flow NASA TM 1–2568 (ICOMP-90-12), NASA Lewis Research Center, 1990.

[15] A.C. Megri, F. Haghighat, Zonal modelling for simulating indoor environment of building: review development and applications, HVAC&R Research 13 (2007) 1–19.

[16] A.C. Megri, M. Snyder, M. Musy, Building zonal thermal and airflow modelling-A review, International Journal of Ventilation 4 (2) (2005) 177–188.

[17] K. Miura, The analysis of a thermal storage system utilizing building mass in a cold region, in: Proceedings of the BS2007, Beijing, China, The 10th International Building Performance Simulation Association Conference and Exhibition, 2007, pp.465–472.

[18] A. Moser, A. Schalin, F. Off, X. Yuan, Numerical modeling of heat transfer by radiation and convection in an atrium with thermal inertia, ASHRAE Transactions 101 (2) (1995) 1136–1143.

[19] M. Peric, R. Kessler, G. Scheuerer, Comparison of finite volume numerical methods with staggered and colocated grids, Computers and Fluids 16 (1988) 389–403.

[20] F. Song, Dynamic Simulation of Atrium Thermal Environment, Master thesis, Tsinghua University, Beijing, China, 2004.

[21] S. Togari, Y. Arai, K. Miura, A simplified model for predicting vertical temperature distribution in a large space, ASHRAE Transactions 99 (part 1) (1993) 84–99.

[22] E. Wurtz, M. Musy, F. Allard, Modélisation d'un panache d'émetteur de chaleur pour le logiciel de simulation énergétique des batiments orientéobjet SPARK, International Journal of Thermal Science 39 (3) (2000) 433–441.

[23] Z. Zhai, Q. Chen, P. Haves, J.H. Klemsb, On approaches to couple energy simulation and computational fluid dynamics programs, Building and Environment 37 (2002) 857–864.